J Infrared Milli Terahz Waves (2014) 35:770–779
DOI 10.1007/s10762-014-0080-1

Terahertz Conductivity and Hindered Molecular Reorientation of Lithium Salt Doped Succinonitrile in its Plastic Crystal Phase

Daniel V. Nickel · Hongtao Bian · Junrong Zheng · Daniel M. Mittleman

Received: 30 April 2014 / Accepted: 21 May 2014 /
Published online: 8 June 2014

Abstract The terahertz complex permittivity of the molecular plastic crystal succinonitrile (SN) or 1,2 dicyanoethane ($N{\equiv}C{-}CH_2{-}CH_2{-}C{\equiv}N$), doped with the lithium salts $LiBF_4$, $LiPF_6$, LiTFSI, and $LiClO_4$ to form solid-state plastic crystal electrolytes, is measured and compared using temperature-dependent terahertz time-domain spectroscopy (THz-TDS). In contrast to the trends at low frequency, SN's terahertz conductivity *decreases* slightly when doped with Li-salts. This indicates that at high frequencies the dielectric response is not dominated by ionic charge transport, but instead by relaxational processes which are hindered by the presence of the ionic dopants. Assuming a single Cole-Cole distribution of Debye-like processes dominates the measured spectra, the average relaxation times τ and Arrhenius activation energies E_a are extracted for each electrolyte and are shown to increase significantly relative to undoped SN's τ and E_a, indicating the relaxational processes are hindered by the presence of the ionic dopants.

Keywords succinonitrile · solid-state electrolytes · plastic crystal · dielectric relaxation · THz-TDS

1 Introduction

Succinonitrile (SN) is a translationally ordered, rotationally disordered molecular plastic-crystal at room temperature which becomes a solid-state electrolyte when doped with different ionic species; the solvated (cat/an) ions can easily diffuse through the static matrix of the plastic-crystal, increasing its DC conductivity by orders of magnitude relative to its intrinsic conductivity [1]. , Given its relatively low melting point (62°C) and high static dielectric constant (ε_0=55) [2], lithium salts commonly used in electrolytic power sources can be easily solvated into molten succinonitrile, making it a relatively simple and inexpensive class of solid-state electrolyte. Hence, there has been continued interest in its use as a host for electrolytic compounds in

D. V. Nickel (✉) · D. M. Mittleman
Department of Electrical & Computer Engineering, Rice University, MS 378, Houston, TX 77005, USA
e-mail: dn4@rice.edu

H. Bian · J. Zheng
Department of Chemistry, Rice University, MS 60, Houston, Texas 77005, USA

solid-state power sources [3-5]. The DC ionic transport in SN-based electrolytes is thought to be facilitated in part by the rotational disorder of its plastic-crystal phase in addition to defects in its crystal lattice [6]. While there have been many studies concerning the long range DC ionic conductivity and low frequency (<3 GHz) dielectric permittivity [7,8] of succinonitrile-based electrolytes, there have been no studies of the behavior of its high frequency (THz range) conductivity, either with or without ionic dopants. Terahertz time-domain spectroscopy (THz-TDS) has been effective in characterizing the high frequency complex conductivities of ionic liquids [9], conductive polymers, and semiconductor nano-materials [10] and is well suited for probing the complex conductivity of this solid-state electrolytic material. In this work, the temperature-dependent complex conductivities of succinonitrile-based electrolytes, i.e. succinonitrile doped with the lithium salts LiTFSI, $LiBF_4$, $LiPF_6$, and $LiClO_4$, are characterized using THz-TDS for frequencies of 0.2 to 1.6THz and temperatures of -35° to 62°C.

2 Methods

The samples are prepared by heating the plastic-crystal succinonitrile (SN), obtained from Sigma-Aldrich chemicals with 99% purity and used without further purification, above its plastic crystal to liquid phase transition. The lithium cation with four different anions: tetrafluoroborate (BF_4^-), hexafluorophosphate (PF_6^-), perchlorate (ClO_4^-), and bis(trifluoromethanesulfonyl)imide ($TFSI^-$), are dissolved into the SN melt with a 0.5 M concentration and stirred at 60 °C under the dry N_2 environment until a homogeneous mixture was obtained. The prepared ionic liquids are then injected into the center of a ring-shaped Teflon spacer which is situated on a 1-mm thick TPX wafer. An identical TPX wafer is then placed on top of the molten solution, effectively sandwiching it between the two wafers. The Teflon spacer, with a thickness that ranged from 500μm to 100μm, is used to insure a constant sample thickness over the entire area of the incident THz beam and, combined with the top wafer, prevents evaporation of the sample while in vacuum. The sample is then allowed to slowly cool back to room temperature. Using this method, a polycrystalline solid is formed between the two wafers. The entire sample is larger than the diffraction-limited spot size of the THz beam, but individual crystallites within the polycrystalline solid are significantly smaller. Thus, the measurements are considered to be an average over all crystal orientations. All the samples are prepared and cooled in a dry N_2 environment to prevent water contamination. For each ionic solute, a minimum of three samples with different optical path lengths (spacers) are measured. The spectra shown here are the averages calculated from all the different measured path lengths.

The prepared samples are placed inside a cryostat which is situated at the focal point of a traditional transmission geometry THz-TDS setup [11]. Inside the cryostat, the sample is held under vacuum (<$1x10^{-4}$ mbar) while outside the THz beam path is purged with dry N_2 to eliminate water vapor absorption lines from the spectra. The complex index of refraction $\tilde{n}(\nu)$ is extracted numerically using the Newton-Raphson method from the measured complex transmission function (the ratio of the Fourier transforms of the THz time-domain waveforms transmitted through the sample and an empty reference). The numerical method is necessary since, for this material, n/κ is not large compared to unity, hence the analytically solvable thick film approximation can not be applied without introducing significant error. Finally, from $\tilde{n}(\nu)$ the complex conductivity and permittivity can be determined since $\tilde{n}^2 = \varepsilon_1 + i\varepsilon_2 = 1 + i\tilde{\sigma}/(\varepsilon_0\omega)$. The Origin software package, which uses the Levenberg-Marquardt algorithm, is used to fit the measured THz spectra to theoretical models. Each fitted curve is a *simultaneous* fit of both the real and imaginary parts of the measured spectra.

3 Results & Discussion

Plotted in Figure 1 are the mean complex conductivity spectra for the undoped and Li-salt doped SN at 20°C. The measured spectra are somewhat reminiscent of the behavior of a solid in which the charge carriers exhibit strong backscattering, as in the Drude-Smith model, with a negative imaginary conductivity [12, 13]. It is immediately clear, however, that the anticipated trend in the real part of the conductivity does not follow as expected from earlier low-frequency and DC measurements [1,2,7]. In particular, as can be seen from the measured conductivity at 750 GHz (Figure 1 inset), the magnitude of the conductivity *decreases* slightly with the addition of ionic dopants. In contrast to these results, the DC and low frequency conductivity of SN in its plastic-crystal phase *increases* by as much as 3 orders of magnitude when doped with the same ionic species [1,2]. Of course, at terahertz frequencies the carrier response is being probed at significantly shorter length and time scales. We can estimate the distance a lithium ion or its anion diffuses through the plastic-crystal matrix before the probing electric field reverses direction using $L_\omega = \sqrt{D/\omega}$, where D is the diffusion coefficient of the charge carrier and ω is the probing frequency [14, 15]. For LiTFSA solvated in solid succinonitrile, $D \approx 10^{-6}$ cm^{2}s^{-1} [1] and with a probing frequency of 1 THz, L_ω is an insignificant 0.01nm. Therefore, over the picosecond duration of the THz pulse, the ionic dopants are essentially motionless. The equivalent Einstein mobility is $eD/k_BT \approx 4\times10^{-5}$ cm^2/Vs, which is far too small to contribute significantly to the dielectric response at these frequencies. We conclude, therefore, that the response in the terahertz range is dominated by relaxational processes. The data of Fig. 1 also suggest a very slight increasing trend in the conductivity of the doped samples which may be correlated with the dissociation constants of the salts in liquid phase SN $\left(K_d^{LiBF_4} < K_d^{LiPF_6} < K_d^{LiTFSI} < K_d^{LiClO_4}\right)$ [16]. However, given the uncertainty in these measurements, additional data are needed to determine if this trend is statistically relevant.

In Figure 2 we plot the same spectra as Figure 1, converted to complex permittivity. The measured decrease in the real part of the conductivity with the addition of Li-salt dopants is reflected in ε_2. Here it is clear the permittivity spectra resemble the behavior of dielectric

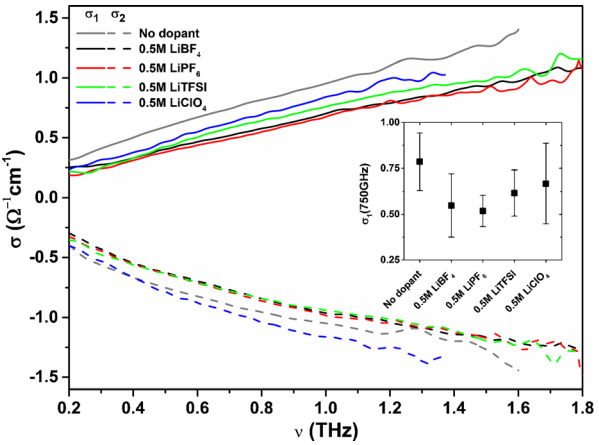

Figure 1 The mean real (solid lines) and imaginary (dashed lines) conductivity spectra at T=20°C of the plastic-crystal succinonitrile: undoped (grey lines) and doped with the various Li-salts at 0.5M concentration (colored lines). Inset: The real part of the conductivity at 750GHz and 20°C for each sample, plotted with the typical error.

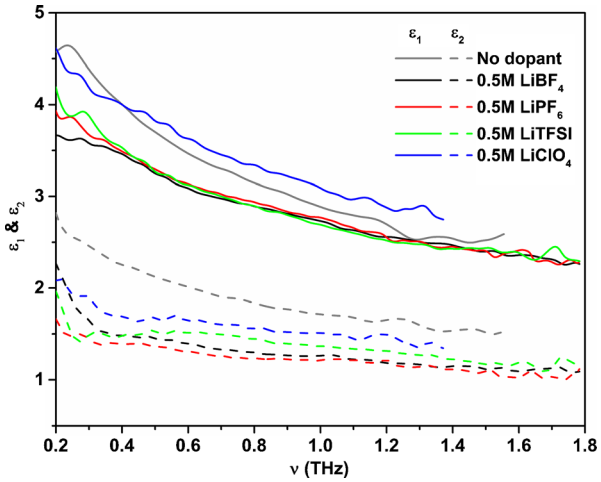

Figure 2 The mean real (solid) and imaginary (dashed) permittivity spectra at 20°C for the undoped (grey) and Li-salt doped succinonitrile samples.

relaxational processes, similar to THz studies of other materials where both ε' and ε" *decrease* with increasing frequency [17-19]; this behavior indicates we may be observing the high frequency wing of a dielectric relaxational process. Considering that SN in its plastic-crystal phase is rotationally disordered, the behavior of its measured THz spectrum is most likely due to the presence of this disorder. Many previous studies, such as dielectric relaxation measurements [20], depolarized Rayleigh scattering [21, 22], optical Kerr effect [23, 24], and incoherent quasi-elastic neutron scattering [25, 26] have revealed the existence of several relaxational processes, one of which can be attributed to the *gauche-trans* isomerisation inherent in the plastic-crystal phase of SN. There are also faster (sub-10 picosecond) timescale *trans-trans* rotational dynamics present in this phase [23-26]. However, these dynamics are undetectable using THz- TDS and dielectric methods since only the *gauche* conformation has a non-zero electric dipole moment. Additionally, in SN's low temperature (< -35°C) rigid crystal phase the Debye-like behavior is frozen out, resulting in THz spectra with comparatively lower dispersion, lower absorption, and characteristic lattice vibrational modes indicative of an orientationally and spatially ordered molecular crystal [27]. Therefore, the behavior of the THz spectra is a direct consequence of the rotational disorder inherent in its plastic-crystal phase.

If we assume the *gauche-trans* reorientational process is the most dominant contribution to the measured THz spectra, we can fit the measured spectra to a simple relaxational model. In Fig. 3, we plot the *simultaneous* fits of both $\varepsilon_1(\nu)$ and $\varepsilon_2(\nu)$ to the Cole-Cole equation [28]:

$$\hat{\varepsilon}(\omega) = \varepsilon_\infty + \frac{\varepsilon_0 - \varepsilon_\infty}{1 + (i\omega\tau)^{1-\alpha}} \quad (1)$$

Here ε_∞ and ε_0 are the high and low frequency permittivity limits respectively, taken from references [29, 30]. The two fit parameters are τ, the characteristic relaxation time, and α, an exponent parameter. When α=0, the Cole-Cole equation reduces to the Debye equation. Here, the inclusion of the extra parameter to the Debye equation can be interpreted as the presence of a continuous distribution of Debye relaxations centered about a single peak value of τ, with α representing the width of this distribution. The Cole-Cole equation results in the best quality of fits to the measured THz spectra

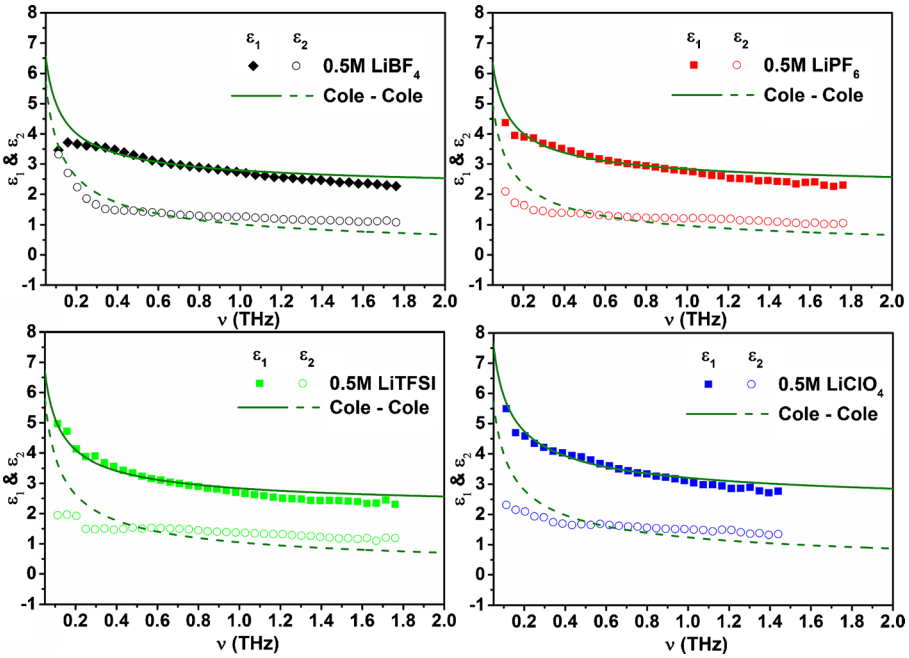

Figure 3 The measured (data points) and fitted Cole-Cole (green lines) complex permittivity spectra for the four Li-salt doped succinonitrile samples at 20°.

assuming a single distribution, with coefficients of determination of $R^2 \approx 0.94$. Other variants of the Debye equation were considered as well, including the three-parameter Havriliak-Negami equation, the two-parameter Cole-Davidson equation and the Debye equation itself, with each resulting in comparatively lower values of R^2. Of course, more phenomological approaches could be used to better fit the spectra. However, in the context of this work the Cole-Cole model adequately describes the data while still maintaining physical significance. Most importantly, the trends in the fitted parameters vs. doping and temperature can be demonstrated.

Plotted in Figure 4 are the extracted mean parameters τ and α for each different set of SN-based electrolyte sample at 20°C. The undoped SN sample set has a mean characteristic relaxation time of 65 ± 17 ps. Given the extracted resonant absorption peaks at τ^{-1} are outside of the measured frequency range, it can be difficult to obtain reliable quantitative values for the fitted parameters. Therefore, in this case, emphasis must be placed on the *trends* in the parameters vs. temperature and dopants rather than their actual values. However, we note that the extracted value of the τ parameter for the undoped SN is in reasonable agreement with all the previously cited studies [20-26], with τ's ranging from 44ps to 64ps. Even so, the most significant result is the notable increase in τ when the ionic dopants are added. We can speculate the presence of the solvated Li-salt cations and anions in the plastic-crystal lattice hinders the relaxational processes. Here, even in the time scale of the longest average relaxation time (τ=207ps) an ion will only diffuse approximately 0.2nm, which is still less than the length of a single unit cell of SN (a=0.637nm) [31]. Finally, the extracted mean values of α are approximately equivalent, independent of doping, indicating their relaxation time distributions have equal widths within the error.

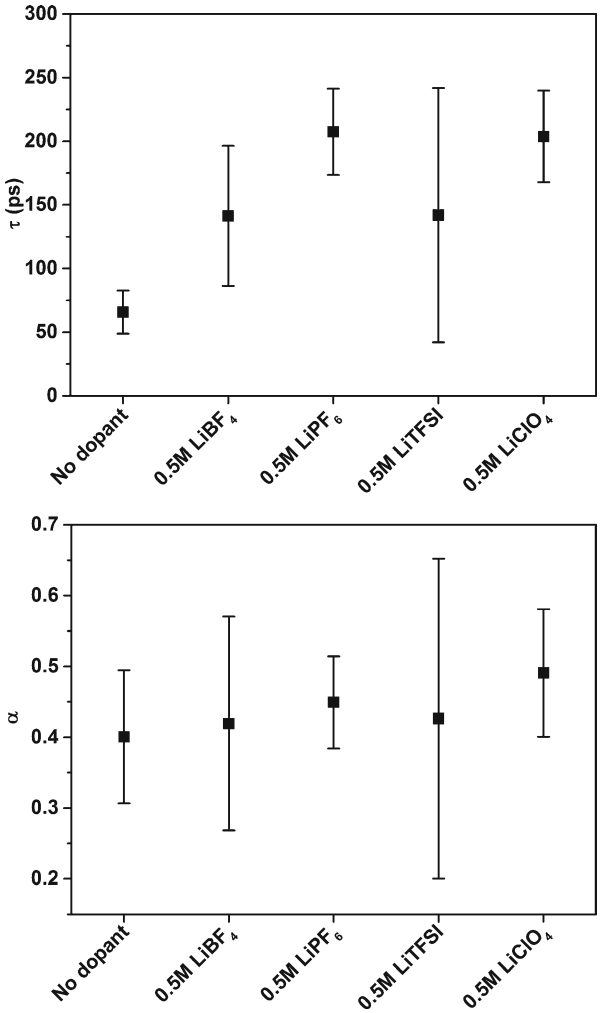

Figure 4 The extracted mean Cole-Cole relaxation times τ and width parameters α for the undoped and Li-salt doped succinonitrile samples at 20°C.

The extracted Cole-Cole relaxation times also display a significant dependence on temperature, with exponentially decreasing τ's as the temperature increases. Figure 5 is an Arrhenius representation of the extracted temperature-dependent relaxation rates for the each of the different SN-based electrolyte samples. Given the linearity of the data, the average activation energies, E_a, of the relaxational processes for each different sample can be extracted using the phenomological Arrhenius equation, $\tau^{-1} = Ae^{-E_a/RT}$. For pure succinonitrile, E_a is approximately 3 kJ/mol, which is lower than the values obtained using other methods. For example, low-frequency dielectric techniques measure E_a to be 10.5 kJ/mol [20] and 11.3 kJ/mol [22], whereas optical Kerr effect methods measure E_a to be 9 kJ/mol [20] and 18 kJ/mol [21]. Additionally, neutron scattering methods measure E_a=26.08 kJ/mol [22] and 15 kJ/mol [23]. Hence, comparatively there is already significant scatter in the measured activation energy between the different methods. Additionally, the extracted values of the pre-exponential factor,

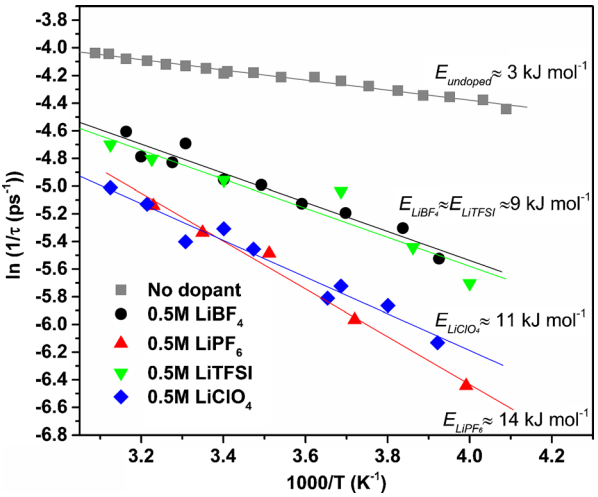

Figure 5 Arrhenius plot of the relaxation rates, i.e. the natural log of the inverse of relaxation times for the different SN-based electrolytes plotted vs. inverse temperature. Notably, the relative activation energies increase when the sample is doped with Li-salts.

A, are on average 0.5 ps^{-1}, which is significantly slower than the rate predicted from transition state theory ($A = k_BT/h \approx 6.2\ ps^{-1}$ at room temperature) [32]. The origin of this discrepancy is unclear, and as noted above the significance of extracted fit parameters should not be overemphasized, given the limited spectral range of the experiment. It is interesting to note that the THz regime partly bridges the gap between the long range, macroscopic response measured by low-frequency dielectric methods and the short range, effectively single molecule response measured by optical Kerr effect and neutron scattering methods. Hence, it is plausible that THz measurements may be probing a subset of mesoscopic modes with lower activation energies compared to other techniques.

Using an alternate approach, the extracted relaxation times can be fit to a modified form of the Arrhenius equation:

$$\tau = \tau_0 + A^{-1} e^{\frac{E_a}{RT}} \tag{2}$$

where an offset, τ_0, is included. When τ_0=0, the reciprocal of the Arrhenius equation is recovered. This analysis is similar to that used in 2-D IR spectroscopy for solute-solvent complex kinetics [33, 34]. Plotted in Figure 6 is a comparison of the extracted energies from the fits using both the Arrhenius equation and Equation 2, including several different choices of A^{-1}: as a temperature-independent free parameter, as h/k_bT, and as $(I/k_bT)^{-0.5}$. Here $(I/k_bT)^{-0.5}$ is the diffusional reorientation time of a free rotor, where I is the rotational inertia of SN's gauche conformation [35], which may be more applicable to this molecular reorientational system. In all cases, the inclusion of the additional offset parameter shifts E_a to higher energies, closer to the values obtained using other methods. Additionally, we can speculate the significant non-zero values of the offsets, τ_0, are a direct result of the inherently hindered rotation of SN's gauche conformation in its plastic-crystal lattice; the *gauche-trans* isomerization is already hindered if its nearest neighbors are in their *gauche* conformations.

Despite the different results obtained using various different fitting procedures, the relative activation energies of the different electrolyte samples can still be compared.

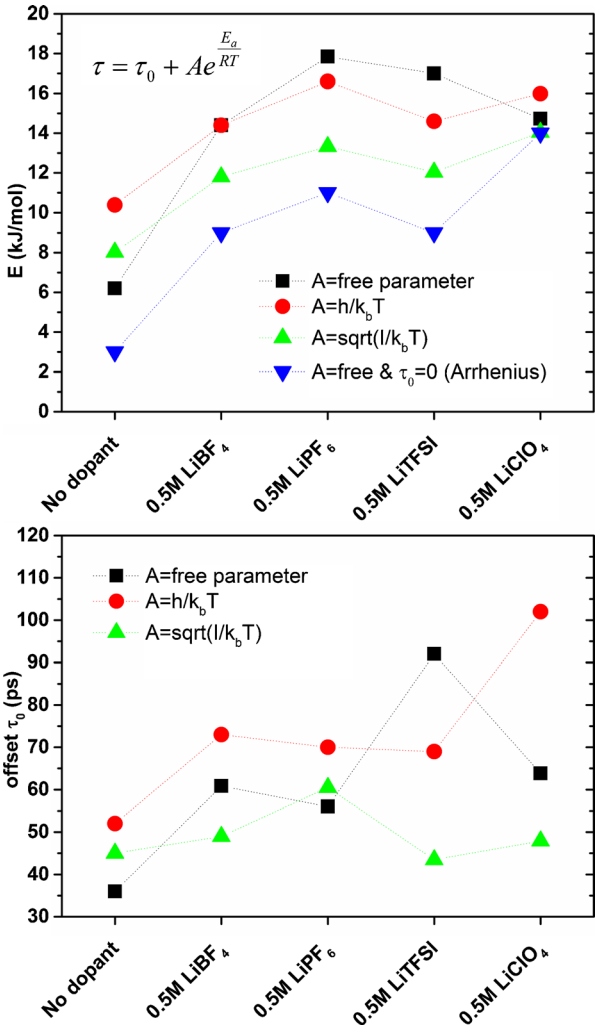

Figure 6 Comparison of the energies E_a and offset τ_0 from Equation 2 using the different pre-factor choices. Most importantly, regardless of the pre-factor choice, in all cases E_a increases when ionic dopants are present.

Most importantly, in *all* cases and regardless of the pre-factor choices, when SN contains ionic impurities the activation energy of the reorientational relaxation increases considerably relative to that of pure SN. The higher activation energies in the doped samples indicates the magnitude of the rotational potential barriers separating SN's different accessible conformations has increased due to the presence of the effectively motionless (on the relevant time scales) ionic impurities in its crystal lattice. In addition, we note that the SN samples doped with $LiPF_6$ and $LiClO_4$ exhibit higher activation energies compared to the other two dopants. This is consistent with XRD studies suggesting that these two anions form periodic crystalline-adduct structures with SN, rather than simply occupying lattice defect sites [2,3]. Thus, their higher E_a's are most likely due to this propensity to associate more highly with SN.

4 Conclusion

The solvated ionic species in this experiment, dispersed throughout SN's plastic-crystal lattice at a 0.5M concentration, have very little effect on its complex conductivity spectrum in the THz range. The slight decrease in the THz conductivity may be due to the predicted increase in the *trans* to *gauche* ratio in SN after Li-salt doping [6]. In contrast to the THz regime, the predicted increase in *trans* conformer concentration is thought to help facilitate long range DC ionic transport and consequently the higher measured DC conductivity. Assuming SN's *gauche-trans* reorientation dominates the THz spectra, the extracted mean relaxation time of pure SN's relaxational process agrees well with previous studies. The extra parameter α of the Cole-Cole equation is most likely needed due to correlated, many-body nature of the mesoscopic relaxational process, which gives rise to an inhomogeneous distribution of relaxation times. Most importantly, there is a clear increasing trend in the fitted parameters after SN is doped with the Li-salts. The presence of the dissolved Li-salt cations and anions in the crystal lattice, which are effectively motionless on the time scale of the THz perturbation and of the rotational relaxation itself, hinder the rotation of the succinonitrile molecules; this is revealed by the considerable *relative* increase of the parameters τ and E_a in the presence of ionic impurities.

Acknowledgements This work was supported by the Welch foundation under Award No. C-1752, and the Air Force Office of Scientific Research under AFOSR Award No. FA9550-11-1-0070. J. R. Zheng also thanks the David and Lucile Packard Foundation for a Packard fellowship.

References

1. Long, S.; MacFarlane D.R.; Forsyth, M. Fast Ion Conduction in Molecular Plastic Crystals. *Solid State Ionics* **2003**, 161, 105-112.
2. Alarco, P.; Abu-Lebdeh, Y.; Abouimrane, A.; Armand, M. The Plastic-Crystalline Phase of Succinonitrile as a Universal Matrix for Solid-State Ionic Conductors. *Nature Materials* **2004**, 3, 476-481.
3. Abouimrane, A.; Whitfield, P.S.; Niketic, S.; Davidson, I.J. Investigation of Li Salt Doped Succinonitrile as Potential Solid Electrolytes for Lithium Batteries. *J. Power Sources* **2007**, 174, 883-888.
4. Pringle, J. M. Recent Progress in the Development and Use of Organic Ionic Plastic Crystal Electrolytes. *Phys. Chem. Chem. Phys.* **2013**, 15, 1339.
5. Das, S.; Bhattacharyya, A. J. Influence of Water and Thermal History on Ion Transport in Lithium Salt-succinonitrile Plastic Crystal Electrolytes. *Solid State Ionics* **2010**, 181, 1732-1739.
6. Das, S.; Prathapa S. J.; Menezes, P.V.; Guru Row T.N.; Bhattacharyya, A.J. Study of Ion Transport in Lithium Perchlorate-Succinonitrile Plastic Crystalline Electrolyte via Ionic Conductivity and in Situ Cryo-Crystallography. *J. Phys. Chem. B* **2009**, 113, 5025-5031.
7. Das, S.; Bhattacharyya, A. J. Dielectric Relaxation Spectroscopy for Evaluation of the Influence of Solvent Dynamics on Ion Transport in Succinonitrile-Salt Plastic Crystalline Electrolytes. *J. Phys. Chem. B* **2011**, 115, 2148-2154.
8. Bauer, T.; Kohler, M.; Lunkenheimer, P.; Loidl, A.; Angell, C. A. Relaxation Dynamics and Ionic Conductivity in a Fragile Plastic Crystal. *J. Chem. Phys.* **2010**, 133, 144509.
9. Brauer, J.C.; Thorsmolle, V.K.; Moser, J.E. Terahertz Time-Domain Spectroscopy Study of the Conductivity of Hole-Transporting Materials. *Chimia* **2009**, 63, 189-192.
10. Lloyd-Hughes, J.; Jeon, T.I. A Review of the Terahertz Conductivity of Bulk and Nano-Materials. *J. Infrared Milli. Terahz. Waves* **2012**, 33, 871-925.
11. Mittleman, D. M. (Ed.) *Sensing with Terahertz Radiation*; Springer: New York, **2003**.
12. Smith, N. V. Classical Generalization of the Drude Formula for the Optical Conductivity. *Phys. Rev. B* **2001**, 64, 155106.
13. Walther, M.; Cooke, D. G.; Sherstan, M.; Hajar, M.; Freeman, M. R.; Hegmann, F. A. Terahertz Conductivity of Thin Gold Films at the Metal-Insulator Percolation Transition. Phys. Rev. B. **2007**, 76, 125408.

14. Henning, P.F.; Homes, C.C.; Maslov, S.; Carr G.L.; Basov, D.N.; Nikolic, B.; Strongin M. Infrared Studies of the Onset of Conductivity in Ultrathin Pb Films. *Phys. Rev. Lett.* **1999**, 83, 4880.
15. Cooke, D. G.; MacDonald, A. N.; Hryciw, A.; Wang, J.; Li, Meldrum, Q. A.; Hegmann, F. A. Transient Terahertz Conductivity in Photoexcited Silicon Nanocrystal Films. *Phys. Rev. B* **2006**, **73**, 193311.
16. Xu, K. Nonaqueous Liquid Electrolytes for Lithium-Based Rechargeable Batteries. *Chem. Rev.* **2004**, 104, 4303-4417.
17. Møller, U.; Cooke, D.G.; Tanaka, K.; Jepsen, P. U. Terahertz Reflection Spectroscopy of Debye Relaxation in Polar Liquids *J. Opt. Soc. Am. B.* **2009**, 9, A113.
18. Koeberg, M.; Wu, C.C.; Kim, D.; Bonn, M. THz Dielectric Relaxation of Ionic Liquid:Water Mixtures *Chem. Phys. Lett.* **2007**, 493, 60-64.
19. Kindt, J.T.; Schmuttenmaer, C.A. Far-Infrared Dielectric Properties of Polar Liquids Probed by Femtosecond Terahertz Pulse Spectroscopy, *J. Phys. Chem.* **1996**, 100, 10373-10379.
20. Clement, C.; Davis, M. Molecular Rotation and Dielectric Relaxation in a Crystal Lattice. *J. Chem. Phys.* **1960**, 32, 316.
21. Boyer, I.; Vacher, R.; Cecchi, I.; Adam, M.; Berge, P. Rayleigh Scattering in a Plastic Crystal Due to Orientational Relaxation. *Phys. Rev. Lett.* **1971**, 26, 1435.
22. Jackson, D. A.; Bird, M. J.; Pentecost, H. T. A.; Powles, J.G. Molecular Reorientation Rates in Crystal By Anistropic Light Scattering. *Phys. Lett.* **1971**, 35A, 1.
23. Ho, P. P.; Alfano, R.R. Relaxation Kinetics of the Plastic Crystal Succinonitrile. *Phys. Rev. A* **1977**, 17, 1161.
24. Foggi, P.; Righini, R.; Torre, R. Angeloni, L.; Califono, S. The Dynamics of Succinonitrile in the Plastic Phase by Subpicosecond Time Resolved Optical Kerr Effect. *J. Chem. Phys.* **1992**, 96, 110.
25. Bee, M.; Lechner, R. E.; Amoureux, J. P.; Fouret, R. Temperature Dependence of Rotational Isomerization and Molecular Reorientation Rates in Plastic Succinonitrile. *J. Phys. C.* **1983**, 16, 4973-4984.
26. Leadbetter, A. J.; Turnbull, A. Molecular Reorientation in Three Orientationally Disordered Molecular Crystals by Incoherent Neutron Scattering. *Soc. Faraday Trans.* **1977**, 73, 1788-1804.
27. Nickel, D.N.; Delaney, S.; Korter, T.M.; Bian, H.; Zheng, J.; Mittleman, D.M. Terahertz Vibrational Modes of the Rigid Crystal Phase of Succinonitrile.. *J. Phys. Chem. A* **2014**, 118, 2442-2446.
28. Cole, K.S.; Cole, R.H. Dispersion and Absorption in Dielectrics - I Alternating Current Characteristics. *J. Chem. Phys.* **1941**, 9, 341.
29. Williams, D.E.; Smyth, C. R. The Dielectric Dispersion of Dibromodichloromethane, Succinonitrile, and Several Camphor Derivatives in the Solid State. *J. Am. Chem. Soc.* **1962**, 84, 1808.
30. *CRC Handbook of Chemistry and Physics.* **2013-2014,** 94th ed. CRC Press: Boca Raton, FL,; p 3-522.
31. Hore, S.; Dinnebier, R.; Wen, W.; Hanson, J.; Maier, J. Structure of Plastic Crystalline Succinonitrile: High-Resolution in situ Powder Diffraction. *Z. Anorg. Allg. Chem.* **2009**, 635, 88-93.
32. Chang, R. Physical Chemistry for the Chemical and Biological Sciences; University Science Books: Sausilito, 2000.
33. Zheng, J.; Fayer, M. D. Solute-Solvent Complex Kinetics and Thermodynamics Probed by 2D-IR Vibrational Echo Chemical Exchange Spectroscopy. *J. Phys. Chem. B.* **2008**, 112, 10221.
34. Zheng, J. R.; Fayer, M. D. Hydrogen bond lifetimes and energetics for solute/solvent complexes studied with 2D-IR vibrational echo spectroscopy. *J. Am. Chem. Soc.* **2007**, 129, 4328-4335.
35. Wroz, T.; Kubicki, J.; Naskrecki, R.; Bancewicz, T. The dynamics of succinonitrile in the plastic and liquid phases from depolarized Rayleigh spectra. *J. Chem. Phys.* **1995**, 103, 9212,